Development of glass fiber-reinforced plastic for orthodontic wires

（グラスファイバー強化プラスチック製歯科矯正ワイヤーの開発）

Toshihiro Inami

Department of Orthodontics,

Nihon University Graduate School of Dentistry at Matsudo

(Director: Prof. Kazutaka Kasai)

Abstract

Generally, orthodontic treatment uses metallic wires made from stainless steel (SS), cobalt-chromium-nickel (Co-Cr), β-titanium (β-Ti), and nickel-titanium (Ni-Ti) alloys. However, these wires are not esthetically pleasing and may induce allergic or toxic reactions. To correct these issues, in the present study glass fiber-reinforced plastic (GFRP) orthodontic wires made from polycarbonate and E-glass fiber were developed by using pultrusion. After fabricating these GFRP round wires with a diameter of 0.45 mm (0.018 inch), their surface characteristics, mechanical and *in vitro* properties were examined. To investigate how the glass-fiber diameter affected their properties, GFRP wires of varying diameters (7 and 13 μm) were prepared. As controls, SS, Co-Cr, β-Ti, and Ni-Ti wires were also evaluated.

Both the GFRP with 13 μm fibers (GFRP-13) and GFRP with 7 μm fibers (GFRP-7) were more transparent than the metallic orthodontic wires. Under scanning electron microscopy and scanning probe microscopy, the surfaces of GFRP wires appeared almost smooth similar to those of SS, Co-Cr, and Ni-Ti, but the surface of β-Ti appeared relatively rough. The dynamic hardness and elastic modulus of GFRP wires obtained by the dynamic micro-indentation method were much lower than those of metallic wires. There was no significant difference in surface properties between GFRP-13 and GFRP-7; presumably because both share the same polycarbonate matrix.

In the results of frictional test, frictional forces of GFRP wires and Ni-Ti were nearly half as low as those of SS, Co-Cr, and β-Ti for two types of esthetic brackets (the polymeric composite brackets or the ceramic brackets). Thus, it was indicated that GFRP wires will deliver superior sliding mechanics with low frictional resistance between the wire and bracket during orthodontic treatment.

By three-point bending test, flexural strengths and moduli of the GFRP wires were nearly equivalent to those of available Ni-Ti wires. GFRP-7 had better flexural properties than GFRP-13, indicating that the flexural properties of GFRP increase with decreasing fiber diameter. Using thermocycling, there was no significant change in the flexural properties of the GFRPs after 600 or 1,200 cycles.

The color changes of GFRPs after 24 h, and following 1, 2, and 4 weeks of coffee immersion at 37°C, were measured by colorimetry. After immersion, both GFRPs showed almost no visible color change. As a result, there were no significant differences in the color difference values or National Bureau of Standards units for GFRP-13 or GFRP-7. Moreover, for both GFRPs, no significant differences were observed in any of the immersion periods. Accordingly, it was indicated that the GFRPs will maintain high color stability during orthodontic treatment. Using a cytotoxicity detection kit, it was found that the glass fiber and polycarbonate components comprising the GFRP were not cytotoxic within the limitations of this study.

In conclusion, it is expected that this metal-free GFRP wire composed of polycarbonate and glass fiber to be useful as an esthetically pleasing alternative to current metallic orthodontic wires.

Key words: Orthodontic wires, Fiber-reinforced composites, Surface characteristics, Mechanical properties, *In vitro* properties

Introduction

Orthodontic wires are widely used as orthodontic appliances throughout treatment. These wires are made from metal alloys such as stainless steel (SS), cobalt-chromium-nickel (Co-Cr), β-titanium (β-Ti), and nickel-titanium (Ni-Ti) alloys [1,2]. Although these wires are strong and durable, they are not esthetically pleasing because of their metallic color, and they have the potential to cause allergic or toxic reactions with the soft or hard tissues of the mouth [3,4]. In response to increasing patient demands, researchers have developed transparent brackets made from ceramics or composites to improve the esthetics of orthodontic appliances [5,6]. They have also developed esthetic archwires made from polymer-coated (Teflon or epoxy resin) alloys as well as glass fiber-reinforced plastic (GFRP) wires [7,8]. The transparent or translucent appearance of GFRP archwires is considered especially attractive. Employed by many industrial fields, GFRPs have been used to fabricate dental appliances such as crowns, bridge, and frameworks for fixed partial dentures in both research and clinical experiments [9-11]. Several reports have also used GFRPs to fabricate orthodontic archwires by combining biocompatible CaO-P_2O_5-SiO_2-Al_2O_3 glass fibers and a matrix of polymethyl methacrylate or urethane dimethacrylate, or an E-glass fiber reinforcement in an epoxy resin matrix [12-14]. These GFRP wires are often much more esthetically pleasing than those made from conventional orthodontic alloys. In general, these GFRP wires are prepared under laboratory conditions. However, it is difficult to precisely control the shape and size of the GFRP wire in the laboratory because the quality of composite materials such as GFRP is affected by the fabrication conditions. Therefore, there is a need to improve the production process of GFRP wire fabrication.

Pultrusion is a commonly used method to industrially fabricate thermoplastic composites [15,16]. This technique is advantageous over other common methods because it can continuously produce profiles in high volumes with a constant cross-section. It is also the fastest and the most cost-effective composite manufacturing process. Among the potential matrix materials for GFRPs, thermoplastics offer substantial advantages over thermosets, including higher toughness and thus higher impact resistance. Polycarbonate is of particular interest because of its high transparency, low weight, and high heat and impact resistance [15,17].

In the present study, esthetic orthodontic wire made from GFRPs composed of glass fiber and polycarbonate was developed by using pultrusion. The mechanical properties and *in vitro* biocompatibility of the GFRPs such as surface characteristics, frictional properties, flexural properties, color stability, and cytotoxicity were evaluated.

Materials and Methods

Materials preparation

GFRP wires were fabricated using pultrusion. A polycarbonate (H4000, Mitsubishi Engineering-Plastics Corp., Tokyo, Japan) was used as the thermoplastic matrix. In this study, this polycarbonate was used because of its low viscosity, which allowed us to fabricate the GFRP wires with diameters as small as those of available orthodontic wires. E-glass fiber filament (Nittobo Co., Fukushima, Japan) was used as unidirectional reinforcement for the polycarbonate matrix. To investigate how fiber diameter affected the GFRP properties, GFRPs with one of two diameters of E-glass fiber were prepared: 13 μm (GFRP-13) or 7 μm (GFRP-7), as shown in Figure 1(a).

Figure 1(b) shows a schematic of the pultrusion facility. From the top to the bottom, the fiber yarns were pulled at 1.3 m/min from a reel through a heated die. The impregnation of the fiber controls the resin content, and curing of the materials into their final shape is completed using the die. The die had a diameter of 0.5 mm and cured the polycarbonate at 295°C. The volume fraction of glass fiber was ~0.3. This fiber fraction was chosen for the present study in order to let the glass-fibers infiltrate into polycarbonate matrix well and prepare a GFRP wire specimen with high elasticity and low stiffness that resist permanent deformation. Thus, the multifilament glass-fibers were well infiltrated into the polycarbonate matrix using pultrusion. From the pultruded samples, round GFRP wire specimens, each with a diameter of 0.45 mm (0.018 inch) and length of 36 cm, were cut. As controls, commercially available orthodontic wires made from SS (Stainless Steel, Ormco, Glendora, CA, USA), a Co-Cr alloy (Elgiloy Red®, Rocky Mountain Orthodontics, Denver, CO, USA), a β-Ti alloy (Bendaloy®,

Rocky Mountain Orthodontics) and two Ni-Ti alloys (Memory Wire, American Orthodontics, Sheboygan, WI, USA; Ni-Ti-A)(Nickel Titanium Straight Lengths, G&H Wire Co., Greenwood, IN, USA; Ni-Ti-B) were prepared in accordance with each test method (Table 1). All specimens were straight round with a diameter of 0.45 mm (0.018 inch).

Surface appearance

The specimen surfaces were vacuum dried and platinum sputtered, and observed under a field-emission scanning electron microscopy (FE-SEM; JSM-6340F, JEOL, Tokyo, Japan) at an accelerating voltage of 5 kV.

Surface topography analysis

Scanning probe microscopy (SPM; SPM-9700; Shimadzu Co., Kyoto, Japan) was performed in the dynamic mode using rectangular silicon cantilevers with a spring constant of ~40 Nm^{-1} and typical resonance frequencies between 250 and 300 kHz. Imaging was accomplished in the attractive tip-sample interaction regime, recording height images, which indicate the distribution of height parameters of the sample's surface. The average surface roughness (R_a) represents the arithmetical mean of the absolute values. The SPM results were obtained as the average values of 5 specimens each (n = 5).

Dynamic micro-indentation test

The mechanical behavior of the GFRP wires was investigated using a dynamic

ultra-micro-hardness tester (DUH-211, Shimadzu) fitted with a Berkovich indenter tip, which is described in detail elsewhere [18]. The specimens were fixed to an attached holder. Dynamic micro-indentation primarily involves applying a controlled load (P) applied through a diamond tip that is in contact with a smooth surface. The penetration depth (h) of indentation is continuously recorded as a function of load. Dynamic hardness and elastic modulus can be obtained from the indentation load and penetration depth data [18,19].

The dynamic hardness (DH) of the sample was calculated from the following equation:

$$DH = \alpha P/h^2, \quad (1)$$

where α is a geometrical constant of the Berkovich indenter (3.8584), P is the applied load during the indentation test, and h is the penetration depth of the indentation.

The elastic modulus (E) of the sample was calculated from the following equation:

$$1 / E_r = (1-V^2)/E + (1-V_i^2)/E_i, \quad (2)$$

where E_r is the reduced elastic modulus from the indenter, V is the Poisson's ratio for the sample, V_i is the Poisson's ratio for the Berkovich indenter (0.07), and E_i is the modulus of the Berkovich indenter (1140 GPa).

In the present study, the dynamic micro-indentation test was carried out with peak loads (P_{max}) of 50 mN. The load rate was kept constant at 13.32 mN/s and the hold time at the maximum load was set to 15 s. The dynamic micro-indentation results, such as dynamic hardness and elastic modulus, were obtained as the average values of 10 specimens each (n = 10).

Frictional test

Frictional behavior of the GFRP wires was measured using a computer-controlled Instron testing machine (TG-5kN; Minebea, Tokyo, Japan) with jig-fixed brackets (Figure 2). Before testing, a jig was prepared using a 195 × 54 × 2.95-mm acrylic plate, on which three brackets (0.022 × 0.028-inch slot) were bonded with cyanoacrylate adhesive. With a slight modification to the technique described by Farronato et al. [20] and Nair et al. [21], the position of three brackets bonded on the acrylic jig was set up. The distance between the three brackets was 8.5 mm, simulating upper right lateral incisor, canine, and first premolar brackets. The central bracket was positioned 1.0 mm more to the left than the other two brackets along a vertical line to have three unaligned horizontal brackets. Two types of esthetic brackets were used: polymeric composite (Silkon, American Orthodontics, Sheboygan, WI, USA) made from short glass fiber-reinforced polycarbonate; and ceramic (Sincere Brace, Kuraray Noritake Dental Inc., Niigata, Japan) made from zirconia. For the friction test, the wires were cut in 18-cm-long segments. The wires were ligated using elastomeric ligatures (Chain Elastic Ligature Clear, American Orthodontics). Testing was performed on an Instron machine with the cross-head speed set at 1 mm/min and the wire pulled through the brackets for 2 min, and the maximum loading as the static friction force was measured with a load cell of 5 kN. A new wire and bracket and a fresh ligature were used for each combination and then discarded to eliminate the influence of wear. The frictional results were obtained as the average values of 10 specimens each (n = 10).

Three-point bending test

Three-point bending tests were performed at a constant loading rate of 1 mm/min with

a span length of 16 mm by using an Instron machine. These specimens were round bars with lengths of 30 mm. The flexural strength F and flexural modulus E were calculated using the following formulae:

$$F = 8PL/\pi d^3 \quad (3)$$

$$E = (4/3)(L^3/\pi d^4)k \quad (4)$$

where P is the maximum load, L is the span length, d is the specimen diameter, and k is the initial slope of the load-deflection curve. The experimental values of the two GFRP wires are averages of 12 specimens each (n = 12). The experimental values of the five metallic wires are averages of 10 specimens each (n = 10).

In addition to these, the loading and unloading tests were performed with the same Instron testing machine that deflected the wires up to 1.95 mm with a crosshead speed of 1 mm/min, and the load-deflection curves of two GFRP wires and five metallic wires were monitored during loading and unloading (n = 3).

Thermal cycling

To test whether the mechanical properties of the GFRPs were stable, GFRPs were thermocycled between 5°C and 55°C in deionized water for 600 or 1,200 cycles by using a thermal cycling machine (Thomas, Tokyo, Japan). In these thermocycling tests, each GFRP was immersed in one bath for 60 s and then transferred to the other bath within 5 s. After thermocycling, the flexural properties were measured again by three-point bending and compared with those before thermocycling; these experimental values are the averages of 12 specimens each (n = 12). In addition, the surfaces of GFRPs were observed after the thermocycling tests by FE-SEM.

Color stability evaluation

The colorimetric measurement of the as-fabricated GFRP wires with such small diameters was impossible; samples with a total width of at least 3 mm are required so that the color can be properly measured by colorimetry, as described later. Accordingly, in the present study, a slight modification to the technique described by da Silva et al. [22] was used to prepare a GFRP sample by tightly arranging seven wire segments (11 mm in length, 0.45 mm in diameter) by fixing both edges with commercially available flowable resin (Filtek^{TM} Flow, 3M ESPE, MN, USA), as shown in Figure 3(a).

GFRP samples were immersed for 4 weeks in 20 mL of coffee (NESCAFE Excella®, Nestlé Japan Ltd., Hyogo, Japan), which was used as a staining solution, in a Teflon-sealed polystyrene bottle at 37°C with the coffee solution refreshed weekly. After staining, the samples were washed with distilled water and dried with paper towels. Color changes after 24 h, and following 1, 2, and 4 weeks of immersion, were measured by a colorimeter (ShadeEye NCC, Shofu Inc., Kyoto, Japan) using a shade tab (A3, SOLARE, GC Corp., Tokyo, Japan), as shown in Figure 3(b). This device contains a pulsed xenon lamp as an optical light source and a three-component silicon photocell as the optical sensor [23]. The colorimetric measurements were performed by contacting the measurement tip of the optical sensor to the GFRP sample using the shade tabs as a reference. The measurement values were obtained as the average of 10 samples (n = 10) with each sample measured three times.

The color parameters were expressed using the Commission Internationale de l'Eclairage (CIE) $L^*a^*b^*$ color space system [24,25], relative to an illuminant standard,

D65. In this three-dimensional color space, the three axes are L^*, a^*, and b^*. The L^* value is a measure of the lightness of an object and is quantified on a scale such that a perfect black has an L^* value of 0 and a perfect reflecting diffuser has an L^* value of 100. The a^* value is a measure of the redness ($+a^*$) or greenness ($-a^*$) of an object, while the b^* value is a measure of the yellowness ($+b^*$) or blueness ($-b^*$) of an object.

The color difference (ΔE^*) before and after immersion, was calculated according to the equation [24]:

$$\Delta E^* = [(\Delta L^*)^2 + (\Delta a^*)^2 + (\Delta b^*)^2]^{1/2} \quad (5)$$

Moreover, the ΔE^* values were converted into National Bureau of Standards (NBS) units by the equation [22,26]:

$$\text{NBS units} = \Delta E^* \times 0.92 \quad (6)$$

These values are shown in Table 2.

Cell culture and cytotoxicity assay

A culture of human gingival fibroblasts (HGFs) from the cellular outgrowth of healthy gingival tissue explants removed from patients undergoing tooth extraction for orthodontic reasons, according to the method of Brunette et al. [27], was established. Informed consent was obtained from all patients before beginning this study, which was conducted according to a protocol reviewed by the ethics committee at the Nihon University School of Dentistry at Matsudo (EC 10-019). After the teeth were extracted, a gingival tissue attached to the interdental papilla was taken and washed twice in phosphate-buffered saline (PBS). The HGFs were maintained in α-minimal essential medium (Wako, Osaka, Japan) supplemented with 100 μg/mL penicillin G (Sigma

Chemical Co, St Louis, MO, USA), 50 μg/mL gentamicin sulfate (Sigma), 0.30 μg/mL amphotericin B (Flow Laboratories, Mclean, VA, USA), and 10% fetal calf serum (Cell Culture Laboratories, Cleveland, OH, USA). The cultures were incubated at 37°C in a humidified incubator (Forma CO_2 incubator MIP-3326, Sanyo Electric Medica System Co., Tokyo, Japan) in 5% CO_2. When the HGFs growing from the explants reached total confluency, they were detached with 0.05% trypsin (Gibco, Grand Island, NY, USA) in PBS for 10 min and then subcultured in flasks. HGFs were seeded at 4×10^4 per well in 96-well culture plates (Sigma) and cultured at 37°C for 24 h.

The cytotoxicity of the glass fibers and polycarbonate comprising the GFRPs were investigated and compared with metallic alloys used for orthodontic wires. Zirconia pieces were used as controls. The HGFs were exposed to the wires in separate wells of 96-well plates (Sigma). Cytotoxicity was determined by a Colorimetric Cell Viability Kit (MTT) (Takara Bio Inc., Shiga, Japan). MTT is a colorimetric assay, which measures the reduction of 3-(4, 5-dimethylthiazol-2-yl)-2, 5-diphenyltetrazolium bromide to a purple formazan product according to the manufacturer's protocol. All samples were cut into 4.0 mm length, and put into the 96-well plates, respectively. Here, fiber sample was applied as multifilament glass-fibers. Then, these were incubated with HGFs for 72 h at 37°C, and the supernatants from these cells were incubated with the substrate mixture and assessed for MTT assay. The purple formazan product from the lysed cells is expressed as the percentage of the control with the mean control value set to 100%. These results are the averages of 4 replicate wells for each test material (n = 4).

Statistical analysis

The experimental results were examined by analysis of variance and Scheffe multiple comparisons test among the means at $p = 0.05$.

Results

Figure 4 shows the appearance and transparency of the GFRPs. Both the GFRP-13 and GFRP-7 wires are more transparent than the available Ni-Ti-A wire. Figure 5 shows FE-SEM images of the surface appearance of the four metallic wires and two GFRP wires. The surfaces of SS, Co-Cr, Ni-Ti-B, GFRP-13, and GFRP-7 appear almost smooth, but the surface of β-Ti appears relatively rough. Figure 6 shows three-dimensional SPM topography images of the tested wires. The average surface roughness of SS, Co-Cr, β-Ti, Ni-Ti-B, GFRP-13, and GFRP-7 was 16.5 ± 8.9, 17.1 ± 2.8, 69.3 ± 10.3, 10.7 ± 2.5, 33.4 ± 8.3, and 20.2 ± 26.6 nm, respectively. The surface roughness of β-Ti observed by SPM is clearly higher than the other wires.

Figure 7(a) shows the dynamic hardness of the tested wires. The dynamic hardness of SS, Co-Cr, β-Ti, Ni-Ti-B, GFRP-13, and GFRP-7 was 444.7 ± 47.4, 449.5 ± 51.7, 355.8 ± 161.4, 228.0 ± 9.2, 13.2 ± 2.2, and 26.0 ± 16.7, respectively. The GFRP wires recorded lower dynamic hardness than the metallic wires ($p < 0.05$). However, there was no significant difference in the dynamic hardness among the GFRP wires ($p > 0.05$), nor among SS, Co-Cr, and β-Ti ($p > 0.05$). Figure 7(b) shows the elastic moduli of the tested wires. The elastic moduli of SS, Co-Cr, β-Ti, Ni-Ti-B, GFRP-13, and GFRP-7 were 135.8 ± 14.5, 152.5 ± 13.1, 90.1 ± 35.6, 46.6 ± 3.2, 2.7 ± 0.8, and 5.7 ± 3.8 GPa, respectively. As in the findings for dynamic hardness, GFRP wires recorded a lower

elastic modulus than metallic wires ($p < 0.05$). Additionally, there was no significant difference in the elastic modulus among the GFRP wires ($p > 0.05$). The standard deviations of dynamic hardness and elastic modulus for β-Ti were larger than those of the other wires owing to the large surface roughness of β-Ti (Figures 5 and 6).

Figure 8(a) shows that the frictional forces of the tested wires against the polymeric composite brackets were 6.92 ± 0.70, 7.18 ± 0.79, 6.56 ± 0.54, 3.87 ± 0.47, 3.45 ± 0.49, and 3.60 ± 0.38 N for SS, Co-Cr, β-Ti, Ni-Ti-B, GFRP-13, and GFRP-7, respectively. The frictional forces of GFRPs and Ni-Ti were significantly lower than those of SS, Co-Cr, and β-Ti ($p < 0.05$). However, there was no significant difference in the frictional forces between the GFRP wires and Ni-Ti wire ($p > 0.05$). Figure 8(b) shows that the frictional forces of the tested wires against the ceramic brackets were 7.53 ± 0.82, 7.62 ± 0.55, 8.66 ± 0.46, 3.47 ± 0.40, 3.39 ± 0.58, and 3.87 ± 0.48 N for SS, Co-Cr, β-Ti, Ni-Ti-B, GFRP-13, and GFRP-7, respectively. For ceramic brackets, there was no significant difference in the frictional forces between the GFRP wires and Ni-Ti wire ($p > 0.05$), and β-Ti recorded the highest frictional force among all the samples ($p < 0.05$).

Figure 9(a) shows the flexural strengths of the tested wires obtained from the three-point bending test. Flexural strengths of SS, Co-Cr, β-Ti, Ni-Ti-A, Ni-Ti-B, GFRP-13, and GFRP-7 were 3547.7 ± 14.0, 3122.5 ± 12.1, 2010.0 ± 47.4, 982.1 ± 18.4, 1019.0 ± 14.4, 690.3 ± 99.2, and 938.1 ± 95.0 MPa, respectively. There were no significant differences in flexural strength among Ni-Ti-A, Ni-Ti-B, and GFRP-7 ($p > 0.05$). Figure 9(b) shows the flexural moduli of the tested wires. Flexural moduli of SS, Co-Cr, β-Ti, Ni-Ti-A, Ni-Ti-B, GFRP-13, and GFRP-7 were 208.0 ± 2.8, 189.5 ± 5.9, 86.2 ± 3.1, 56.2 ± 2.9, 71.8 ± 3.2, 25.4 ± 4.9, and 34.7 ± 7.7 GPa, respectively. There

were no significant differences in flexural modulus between the GFRPs ($p > 0.05$). Figure 10 shows the typical load-deflection curves taken from bending orthodontic wires to 1.95 mm. The wires were deflected to 1.95 mm at their midspan while continuously monitored the force during loading and unloading. In all load-deflection curves, load increased as deflection increased. The load-deflection curves of the SS and Co-Cr wires were linear up to ~0.6 mm. When deflected more than 0.6 mm, its slope gradually decreased. The permanent deflections of the SS, Co-Cr, and β-Ti wires after unloading were approximately 0.25, 0.25, and 0.1 mm, respectively. In contrast, Ni-Ti-A, Ni-Ti-B, GFRP-13, and GFRP-7 wires exhibited no permanent deflection after loading to 1.95 mm and unloading. Figure 11 shows the flexural properties of the GFRPs after thermocycling. After 1,200 cycles, the flexural strength and modulus of GFRP-13 were 651.4 ± 99.0 MPa and 24.9 ± 3.8 GPa, respectively; the flexural strength and modulus of GFRP-7 were 922.4 ± 67.3 MPa and 34.3 ± 5.2 GPa, respectively. Both GFRP-13 and GFRP-7 exhibited no significant differences in flexural properties between 0, 600, and 1,200 thermocycles ($p > 0.05$). Figure 12 shows FE-SEM images of surfaces on GFRPs before and after thermocycling of 1,200 times. No large differences in surface appearances of GFRPs were observed between before and after thermocycling tests.

Figure 13 shows photographs of the GFRP wires before and after 4 weeks of immersion in the coffee solution. After immersion, the GFRP wires showed almost no color change upon visual inspection. Table 3 shows the color differences reported using the ΔE^* and NBS units for the GFRP wires after each immersion period. The ΔE^* values at 24 h and 1, 2, and 4 weeks after immersion for GFRP-13 and GFRP-7 ranged from

0.73 to 1.16 and from 0.62 to 1.10, respectively. There were no significant differences in ΔE^* among any of the measured values for either of the GFRP wires ($p > 0.05$). The NBS units at 24 h and 1, 2, and 4 weeks after immersion for GFRP-13 and GFRP-7 ranged from 0.67 to 1.06 and from 0.57 to 1.01, respectively; as a result, all of the samples exhibited color changes according to the NBS values, which ranged from 0.57 to 1.06. As shown in Table 2, the color change values after immersion for 24 h and 1, 2, and 4 weeks were <1.5 for both GFRPs, and only "slight" color changes were observed according to the NBS units. Furthermore, there were no significant differences in the color-change values for the GFRPs in any of the immersion periods ($p > 0.05$).

Figure 14 shows the results of cytotoxicity experiments after 72 h. The MTT activity of SS, Co-Cr, β-Ti, and Ni-Ti-A wires, as well as of the glass fiber and polycarbonate components of the GFRP wires, were 88.4 ± 13.7, 86.8 ± 2.8, 90.9 ± 9.6, 91.8 ± 9.5, 92.9 ± 11.7, and 95.2 ± 14.0% of controls (control = 100%), respectively. There was no significant difference in cytotoxicity between the GFRP components and the control ($p > 0.05$).

Discussion

To meet the increasing demand for esthetic dental appliances, clinically and esthetically adequate dental materials must be developed. This study aimed to develop esthetic orthodontic archwires by pultrusion of glass fiber-reinforced polycarbonate composites.

The GFRPs had transparency compared with the available Ni-Ti wire (Figure 4). In a clinical setting, transparent or translucent GFRPs are desirable because they can

transmit the color of the host teeth. The main disadvantage of metallic orthodontic wire is usually the metal's opaque, dark appearance, which causes many patients to give up orthodontic treatment [7].

The surface characteristics of orthodontic wires are an essential factor in determining the effectiveness of arch wire-guided tooth movement. In the present study, both FE-SEM and three-dimensional SPM analyses confirmed that the surface roughness of β-Ti is clearly higher than that of other metallic wires and GFRP wires (Figures 5 and 6). These results are consistent with experimental studies of orthodontic wires reported by other researchers [28,29]. The high surface roughness of β-Ti is attributed to adherence or cold welding by the titanium to the dies or rollers during wire processing [30].

The dynamic hardness and elastic modulus of GFRP wires obtained by the dynamic micro-indentation method were notably lower than those of the metallic wires (Figure 7). This is in contrast to the results of three-point bending test, which indicated that the flexural properties of GFRP wires are similar to those of Ni-Ti wires. These results can be explained by differences in the experimental procedures used for evaluating GFRPs and the heterogeneity of GFRPs. Mechanical characterization of orthodontic materials has generally been evaluated using different mechanical testing techniques [31]. The three-point bending test provides a good simulation of orthodontic wires under clinical conditions, and determines the maximal stress and the material's stiffness when a flexural load is applied to bulk materials. In short, this method evaluates the bulk parameters of GFRPs, such as the flexural strength and the flexural modulus. Meanwhile, micro-indentation is a depth-sensing technique that can accurately characterize the surface properties of materials on a small scale. In short, this method

evaluates the surface parameters of GFRPs, such as the dynamic hardness and the elastic modulus. GFRPs are heterogeneous composite materials composed of glass-fiber reinforcement and a polycarbonate matrix. Heterogeneity of GFRPs is an important consideration, because continuous unidirectional GFRPs are anisotropic with high strength and stiffness in longitudinal direction [32,33]. Consequently, GFRPs offer high strength and high stiffness when the optimal combination of reinforcement fiber and matrix resin is used. However, the surface of the GFRPs used in the present study is the polycarbonate matrix, because most of the glass fiber reinforcement is embedded in the polycarbonate (Figure 5). Accordingly, GFRP wires with a polymeric surface (polycarbonate matrix) have significantly lower external surface characteristics than metallic wires. Meanwhile, it is reported that the elastic moduli of polycarbonate obtained by the indentation method were 2.6-2.7 GPa [34]. In this study, the elastic moduli of GFRPs were 2.7-5.7 GPa by the indentation method. This means that depending on where the indenter is pressed (i.e., either a matrix rich area or a fiber rich area), mechanical properties will be different [35].

From the above-mentioned results, it is concluded that the fiber reinforcement does not affect the external surface characteristics, such as dynamic hardness and elastic modulus, obtained by the micro-indentation method, but does affect the solid mechanics, such as flexural strength and modulus, obtained by the flexural test.

In terms of biomechanics, the frictional properties of orthodontic wires are an important parameter in achieving optimal tooth movement. In the present study, for both bracket types (polymeric composite and ceramic), the frictional forces of SS, Co-Cr, and β-Ti wires were nearly twice as high as those of Ni-Ti-B, GFRP-13, and

GFRP-7 wires (Figure 8). Previous studies have indicated that there is a correlation between friction and surface roughness. The surface of β-Ti appeared rough and exhibited high values for friction at the wire-bracket interface [28,29,36]. In this study, it was confirmed that β-Ti wires had a rough surface and high frictional force. However, SS and Co-Cr also recorded high frictional forces, despite having a relatively smooth surface. It is thought that the frictional force values are affected not only by surface roughness, but also by the physical properties of the bulk material, such as stiffness. Contact force keeps adhering the two surfaces (i.e., the wire and the bracket) during sliding in the frictional test; and this increase as the material's stiffness increases [37]. Both SS and Co-Cr alloys have similarly high stiffness. Therefore, it was speculated that the high frictional forces exhibited are due to the high stiffness of SS and Co-Cr and the high surface roughness of β-Ti. In comparison with these alloys, GFRPs and Ni-Ti-B have low surface roughness and low stiffness [30], and thus recorded low frictional forces between the wire and the bracket. The combination of a β-Ti wire and a ceramic bracket recorded the highest friction force of all the combinations of wires and brackets (Figure 8). Orthodontic brackets made from polymeric composites and ceramics have been developed for use as esthetic brackets in clinical situations [5,38]. A polymeric composite bracket (Silkon), made from short glass fiber-reinforced polycarbonate, and a ceramic bracket (Sincere Brace), made from zirconia, were applied in this frictional test. Several reports have investigated the combinations between orthodontic wires and brackets [21,36,38]. Nishio et al. [36] investigated the differences in the frictional forces generated by ceramic brackets, ceramic brackets with a metal-reinforced slot, and SS brackets in combination with SS, Ni-Ti, and β-Ti

archwires. The authors reported that β-Ti wire with its rough surface recorded the highest statistically significant frictional force in comparison with Ni-Ti and SS wires, and the combination of β-Ti wire and a ceramic bracket had the highest frictional force. It is generally known that ceramic brackets cause increased friction during sliding mechanics [39]. Minimizing the friction between the wire and bracket during orthodontic tooth movement is important for optimum orthodontic treatment. Taking these aspects into account, it is expected that the GFRP wires will deliver superior sliding mechanics with low frictional resistance between the wire and bracket during orthodontic treatment. Additionally, there was no significant difference in surface properties between GFRP-13 and GFRP-7, because the surface of both GFRP wires consists of the same polycarbonate matrix.

In the present study, it was examined that the mechanical properties of the GFRP wires in a bending mode because it is more representative of clinical use. These results show that the GFRP wires had similar flexural properties to the Ni-Ti wire (Figure 9). Both Ni-Ti and GFRP deformed elastically when subjected to an intermediate deflection of 1.95 mm and exhibited no permanent deflection upon unloading (Figure 10). It is well-known that in contrast to other alloys such as SS and Co-Cr alloy, Ni-Ti alloys have superelastic properties that resist permanent deformation over a wide range of deflection [1,2]. Additionally, histologic studies on tooth movement have shown that light, continuous, nearly constant forces are optimal in orthodontics. Thus, Ni-Ti wires can deliver optimal orthodontic forces because of its high springback and low stiffness. As shown in Figure 10, the GFRP wires had excellent elasticity and low stiffness, similar to those of the Ni-Ti wires.

The flexural properties of GFRP-7 were better than those of GFRP-13, indicating that the flexural properties of GFRPs improve as fiber diameter decreases. This phenomenon occurs because the number of defects in a fiber decreases as the fiber diameter decreases [40,41]. Additionally, the fiber/matrix interface plays a key role in determining the mechanical behavior of GFRPs. In other words, the most important feature in flexural properties of GFRP is good stress-transfer ability at the fiber/matrix interface. Accordingly, GFRPs derive their strength from the modulus and strength of the fibers embedded in the matrix, which are significantly greater than those of the matrix alone. Because these properties can be tuned by changing the parameters of the fiber (e.g., fiber type, volume fraction, and diameter) as well as by optimizing the stress-transfer ability at the fiber/matrix interface [33], GFRPs may be used during all phases of orthodontic treatment.

Thermocycling test was used to assess the durability of GFRPs in the present study. The results of thermocycling show no significant differences in the flexural properties of GFRPs after 600 or 1,200 cycles (Figure 11). Additionally, there were no large differences in surface appearances of GFRPs before and after thermocycling tests (Figure 12). Therefore, it is thought that there was not degradation of GFRPs after thermal cycling. Several studies have investigated thermal cycling of orthodontic appliances [42,43]. Thermal cycling is a well-known *in vitro* durability test; however, it cannot simulate real clinical conditions. To overcome this limitation, Faltermeier et al. [44] evaluated the mechanical properties of an experimental fiber-reinforced bracket material in a device that simulated the temperature changes and moisture of saliva in the oral environment. They reported that glass-fiber reinforcement can improve the

mechanical properties of polymeric brackets while withstanding the moisture of the saliva in the oral cavity. From the results of this durability tests and those of other researchers, it is speculated that the mechanical properties of GFRPs will remain stable over the course of orthodontic treatment.

GFRP wires are much more esthetically pleasing than wires made from conventional orthodontic alloys because of their transparency. It is difficult for the naked human eye to discern the small-order color changes. Additionally, there are only a few experimental studies on the color stability of esthetic wires because of the small geometry (i.e., shape and dimension) of orthodontic wires and the currently available GFRP wires. Here, by applying the same methods as those used by other researchers [22], a measurement method for determining the color stability of GFRP wires was devised, i.e., colorimetric measurements were performed on GFRP samples prepared by arranging seven wire segments together, as shown in Figure 3(a). Consequently, the color stability of GFRP wires was able to be evaluated according to two evaluation units (ΔE^* and NBS).

First, color differences were assessed by determining the ΔE^* values of the GFRPs after immersion in coffee using the CIE Lab system. The advantage of this system is that color differences can be expressed in units that may be related to visual perception.

There are numerous studies on the threshold levels for the color differences of orthodontic appliances that are visually perceptible or clinically acceptable, and these threshold levels have been assessed using various standards [22,26,45-48]. For example, Douglas et al. [49] reported that the predicted value at which 50% of dentists could perceive a color difference was 2.6 ΔE^* units. In any case, all of the experimental values

obtained for the GFRPs in the present study were lower than 1.5 ΔE^* units, ranging from 0.62 to 1.16 (Table 3). Although evaluating the color changes of orthodontic appliances according to ΔE^* units have not yet been clearly defined, the relatively low ΔE^* values for the present GFRPs suggest that discoloration will not occur during orthodontic treatment.

In addition to using the ΔE^* values, the degree of color differences in GFRPs were assessed in NBS units. According to the critical levels for color differences, both GFRPs underwent "slight" color changes after 4 weeks of immersion in the coffee solution with NBS units ranging from 0.57 to 1.06 (Table 3). Results obtained in NBS and ΔE^* units indicated that both of the GFRPs prepared in this study showed high color stability. Conversely, it has been reported that commercially available GFRPs exhibit "extremely marked" ("much") color change as measured in NBS units after immersion in a coffee solution for 3 weeks at 37°C [22]. The difference in color stability may be explained by differences in the matrix components of the GFRPs. In the present study, the GFRP orthodontic wires were fabricated using polycarbonate as the matrix and glass fiber as reinforcement via pultrusion. In contrast, commercially available GFRPs are typically composed of polymethylmethacrylate (PMMA) and glass fiber [50]. Polycarbonates are generally recognized as low sorption materials [51] and are widely used in orthodontic appliances such as esthetic brackets and clear retainers [39,52]. In particular, Hamanaka et al. [51] reported that polycarbonates have low sorption compared with PMMA, although this research was focused on denture base resins. Additionally, in some articles pertaining to the color stability of brackets, polycarbonate-based brackets showed lower color changes among esthetic plastic

brackets [47]. There is also a known correlation between the color stability and water sorption of a resin [53,54]. Therefore, it is thought that the lower sorption and color changes exhibited by GFRP fabricated in this study compared with commercially available GFRPs are owed to the polycarbonate matrix resin, which keeps the water sorption suitably low for use in orthodontic wire materials. Furthermore, it is worth noting that the flowable resins that used to prepare the samples showed visible discoloration despite the GFRP wires showing no discoloration during the immersion period (Figure 13). Flowable resins are typically composed of dimethacrylates such as bisphenol-A-glycidyl methacrylate and triethylene glycol dimethacrylate (TEGDMA) [55]. It has been reported that materials containing TEGDMA show higher discoloration values because of its hydrophilic property [56]. Therefore, it is speculated that using polycarbonate as the matrix of GFRP fabricated in this study is advantageous because of its higher color stability compared to both TEGDMA and PMMA. In conclusion, the GFRPs fabricated in the present study may be satisfactory for clinical duration of orthodontic treatment in terms of color stability.

As shown in Figure 14, neither the glass fiber nor polycarbonate that comprised the GFRP were cytotoxic compared with the control. The polycarbonate is derived from bisphenol-A. Several studies have evaluated the cytotoxicity of polycarbonate when used as an orthodontic material [57-59]. For example, Kloukos et al. [58] evaluated how water eluents from polycarbonate-based esthetic orthodontic brackets affected the local biological environment. They reported that some polycarbonate-based composite brackets, when exposed to water, released substances that caused mitochondrial apoptosis. Although the cell assay results of the present study indicate that GFRP is not

cytotoxic, more research regarding biocompatibility of GFRP made from polycarbonate and glass fiber must be performed before it can be used in clinical applications.

Finally, compared with metal alloys, GFRPs have several advantages in orthodontic applications, including their esthetics, lack of galvanic corrosion, reduced toxicity compared with diffusing metallic ions, and reduced distortion of magnetic resonance imaging. Pultrusion can prepare GFRP wires with good uniformity and reproducible properties. Therefore, I expect the GFRP wires to be useful alternatives to current metallic wires in future orthodontic treatment (Figure 15).

Conclusions

In this study, metal-free GFRP wires made from polycarbonate and E-glass fiber by pultrusion were prepared for use in esthetic orthodontic appliances. The following conclusions were drawn:

1) The GFRP wires have good transparency compared with other available orthodontic wire alloys.

2) FE-SEM and three-dimensional SPM analysis confirmed that the surface roughness of β-Ti is clearly higher than that of other metallic wires and GFRP wires. Meanwhile, GFRP wires appeared almost smooth similar to SS, Co-Cr and Ni-Ti.

3) Dynamic micro-indentation test revealed no significant differences in the surface properties between GFRP-13 and GFRP-7. This is because the surface of both GFRP wires consists of the same polycarbonate matrix.

4) The frictional forces of GFRP wires were nearly half as low as those of SS, Co-Cr and β-Ti. It was suggested that GFRP wires will deliver superior sliding mechanics with

low frictional resistance between the wire and bracket during orthodontic treatment.

5) The GFRP wires showed bending behavior that is similar to Ni-Ti wires and can deliver optimal and continuous force to teeth because of a high springback and low stiffness. Moreover, there were no significant differences in flexural properties of GFRP before and after thermocycling.

6) The color changes in the GFRPs were minimal during the 4 weeks of coffee immersion. There were no significant differences in the ΔE^* values or NBS units for either GFRP-13 or GFRP-7. Moreover, there were no significant differences for either of the GFRPs for any of the immersion periods. These results indicate that the esthetic properties of GFRPs may remain stable during orthodontic treatment.

7) By using a cytotoxicity detection kit, the glass fiber and polycarbonate components comprising the GFRP were found to be non-cytotoxic within the limitations of this study.

8) The GFRP wires composed of polycarbonate and glass fiber are attractive for orthodontic appliances because of their improved esthetic quality compared with conventional alloys.

Acknowledgments

This article is based on a main reference paper titled, “Surface topography, hardness, and frictional properties of GFRP for esthetic orthodontic wires” in press (2015 Jan28. doi:10.1002/jbm.b.33372) at the *Journal of Biomedical Materials Research Part B: Applied Biomaterials*, and reference papers titled, “Color stability of laboratory glass-fiber-reinforced plastics for esthetic orthodontic wires” in press at the *Korean*

Journal of Orthodontics, "Preparation, mechanical and in vitro properties of glass fiber-reinforced polycarbonate composites for orthodontic application" in press (2014 Jul23. doi:10.1002/jbm.b.33245) at the *Journal of Biomedical Materials Research Part B: Applied Biomaterials*.

References

1. O'Brien WJ: Orthodontic wire. In: O'Brien WJ editor. Dental materials and their selection fourth edition. Chicago: Quintessence Publishing, p 276-292, 2008.
2. Eliades T: Dental materials in orthodontics. In: Graber LW, Vanarsdall Jr. RL, Vig KWL, editors. Orthodontics current principles and techniques fifth edition. Philadelphia: Elsevier, p 1023-1037, 2012.
3. Hensten-Pettersen A, Jacobsen N: Disintegration of orthodontic appliances. In: Eliades G, Eliades T, Brantley WA, Watts DC, editor. Dental materials in vivo aging and related phenomena. Chicago: Quintessence Publishing, p 132-136, 2003.
4. Eliades T, Athanasiou AE: In vivo aging of orthodontic alloys: Implication for corrosion potential, nickel release, and biocompatibility. Angle Orthod, 72:222-237, 2002.
5. Yu B, Lee YK: Aesthetic color performance of plastic and ceramic brackets - an in vitro study. J Orthod, 38:167-174, 2011.
6. Lee YK: Color and translucency of tooth-colored orthodontic brackets. Eur J Orthodont, 30:205-210, 2008.
7. Elayyan F, Silikas N, Bearn D: Ex vivo surface and mechanical properties of coated orthodontic archwires. Eur J Orthodont, 30:661-667, 2008.
8. Ohtonen J, Vallittu PK, Lassila LVJ: Effect of monomer composition of polymer matrix on flexural properties of glass fibre-reinforced orthodontic archwire. Eur J Orthodont, 35:110-114, 2013.
9. Fujihara K, Teo K, Gopal R, Loh PL, Ganesh VK, Ramakrishna S, Foong KWC, Chew CL: Fibrous composite materials in dentistry and orthopaedics: review and

application. Compos Sci Technol, 64:775-788, 2004.

10. Behr M, Rosentritt M, Handel G: Fiber-reinforced composite crowns and FPDs: a clinical report. Int J Prosthodont, 16:239-243, 2003.
11. Monaco C, Ferrari M, Miceli GP, Scotti R: Clinical evaluation of fiber-reinforced composite inlay FPDs. Int J Prosthodont, 16:319-325, 2003.
12. Imai T, Watari F, Yamagata S, Kobayashi M, Nagayama K, Toyoizumi Y, Nakamura S: Mechanical properties and aesthetics of FRP orthodontic wire fabricated by hot drawing. Biomaterials, 19:2195-2200, 1998.
13. Suwa N, Watari F, Yamagata S, Iida J, Kobayashi M: Static-dynamic friction transition of FRP esthetic orthodontic wires on various brackets by suspension-type friction test. J Biomed Mater Res B, 67:765-771, 2003.
14. Huang ZM, Gopal R, Fujihara K, Ramakrishna S, Loh PL, Foong WC, Ganesh VK, Chew CL: Fabrication of a new composite orthodontic archwire and validation by a bridging micromechanics model. Biomaterials, 24:2941-2953, 2003.
15. van Rijswijk K, Bersee HEN: Reactive processing of textile fiber-reinforced thermoplastic composites – An overview. Compos Part A-Appls, 38:666-681, 2007.
16. Gadam SUK, Roux JA, McCarty TA, Vaughan JG: The impact of pultrusion processing parameters on resin pressure rise inside a tapered cylindrical die for glass-fibre/epoxy composites. Compos Sci Technol, 60:945-958, 2000.
17. Van de Velde K, Kiekens P: Themoplastic pultrusion of natural fibre reinforced composites. Compos Struct, 54:355-360, 2001.
18. Nagai M, Tanimoto Y, Inami T, Yamaguchi M, Nishiyama, Kasai K: Effects of indentation load on the mechanical behavior of orthodontic wire alloys by dynamic

micro-indentation method. Int J Oral-Med Sci, 12:41-48, 2013.

19. Sahin O, Uzun O, Sopicka-Lizer M, Gocmez H, Kölemen U: Dynamic hardness and elastic modulus calculation of porous SiAlON ceramics using depth-sensing indentation technique. J Eur Ceram Soc, 28:1235-1242, 2008.
20. Farronato G, Maijer R, Carìa MP, Esposito L, Alberzoni D, Cacciatore G: The effect of Teflon coating on the resistance to sliding of orthodontic archwires. Eur J Orthod, 34:410-417, 2012.
21. Nair SV, Padmanabhan R, Janardhanam P: Evaluation of the effect of bracket and archwire composition on frictional forces in the buccal segments. Indian J Dent Res, 23:203-208, 2012.
22. da Silva DL, Mattos CT, de Araújo MV, de Oliveira Ruellas AC: Color stability and fluorescences of different orthodontic esthetic archwires. Angle Orthod, 83:127-132, 2013.
23. Yamanel K, Gaglar A, Özcan M, Gulsah K, Bagis B: Assessment of color parameters of composite resin shade guides using digital imaging versus colorimeter. J Esthet Restor Dent, 22:379-388, 2010.
24. O'Brien WJ: Color and appearance. In: O'Brien WJ, editor. Dental Materials and Their Selection, 4th ed. Chicago: Quintessence, p 25-37, 2008.
25. Joiner A: Tooth colour: a review of the literature. J Dent, 32:3-12, 2004.
26. Filho HL, Maia LH, Araújo MV, Eliast CN, Ruellas AC: Colour stability of aesthetic brackets: ceramic and plastic. Aust Orthod J, 29:13-20, 2013.
27. Brunette DM, Kenner GS, Gould TR: Grooved titanium surfaces orient growth and migration of cells from human gingival explants. J Dent Res, 62:1045-1048, 1983.

28. Krishnan V, Kumar KJ: Mechanical properties and surface characteristics of three archwire alloys. Angle Orthod, 74:825-831, 2004.
29. Juvvadi SR, Kailasam V, Padmanabhan S, Chitharanjan AB: Physical, mechanical, and flexural properties of 3 orthodontic wires: An in-vitro study. Am J Orthod Dentofacial Orthop, 138:623-630, 2010.
30. Brantly WA: Orthodontic wires. In: Brantly WA, Eliades T, editors. Orthodontic materials. New York: Thieme; p 77-103, 2001.
31. Brantly WA, Eliades T, Litsky AS: Mechanics and mechanical testing of orthodontic materials. In: Brantly WA, Eliades T, editors. Orthodontic materials. New York: Thieme; p 27-47, 2001.
32. Chong KH, Chai J: Strength and mode of failure of unidirectional and bidirectional glass fiber-reinforced composite materials. Int J Prosthodont, 16:161-166, 2003.
33. Tanimoto Y, Nishiwaki T, Nemoto K: Numerical failure analysis of glass-fiber-reinforced composites. J Biomed Mater Res Part A, 68:107-113, 2004.
34. Lorenzo V, de la Orden MU, Munoz C, Serrano C, Martinez Urreaga J: Mechanical characterization of virgin and recovered polycarbonate based nanocomposites by means of Depth Sensing Indentation meaurements. Euro Polym J, 55:1-8, 2014.
35. Drummond JL: Nanoindentation of dental composites. J Biomed Mater Res Part B, 78:27-34, 2006.
36. Nishio C, da Motta AFJ, Elias CN, Mucha JN: In vitro evaluation of frictional forces between archwires and ceramic brackets. Am J Orthod Dentofacial Orthop, 125:56-64, 2004.
37. D'Antò V, Rongo R, Ametrano G, Spagnuolo G, Manzo P, Martina R, Paduano S,

Valletta R: Evaluation of surface roughness of orthodontic wires by means of atomic force microscopy. Angle Orthod, 82:922-928, 2012.

38. Reicheneder CA, Baumert U, Gedrange T, Proff P, Faltermeier A, Muessig D: Frictional properties of aesthetic brackets. Eur J Orthod, 29:359-365, 2007.
39. Eliades T, Eliades G, Brantly WA: Orthodontic brackets. In: Brantly WA, Eliades T, editors. Orthodontic materials. New York: Thieme; p 143-172, 2001.
40. Thomason JL: The influence of fibre length, diameter and concentration on the strength and strain to failure of glass fibre-reinforced polyamide 6,6. Compos Part A-Appls, 39:1618-1624, 2008.
41. Li VC, Obla K: Effect of fiber diameter variation on properties of cement-based matrix fiber reinforced composites. Compos Part B-Eng, 27:275-284, 1996.
42. Bandeira AMB, dos Santos MPA, Pulitini G, Elias CN, da Costa MF: Influence of thermal or chemical degradation on the frictional force of an experimental coated NiTi wire. Angle Orthod, 81:484-489, 2011.
43. Catalbas B, Uysal T, Nur M, Demir A, Bunduz B: Effects of thermocycling on the degree of cure of two lingual retainer composites. Dent Mater J, 29:41-46, 2010.
44. Faltermeier A, Rosentritt M, Faltermeier R, Müßig D: Influence of fibre and filler reinforcement of plastic brackets: an in vitro study. Eur J Orthodont, 29:304-309, 2007.
45. Faltermeier A, Behr M, Müssig D: In vitro colour stability of aesthetic brackets. Eur J Orthod, 29:354-358, 2007.
46. Kim SH, Lee YK: Measurement of discolouration of orthodontic elastomeric module with a digital camera. Eur J Orthod, 31:556-562, 2009.

47. Lee YK: Change in the reflected and transmitted color of esthetic brackets after thermal cycling. Am J Orthod Dentofacial orthop, 133:641.e1-6, 2008.
48. Faltermeier J, Simon P, Reicheneder C, Proff P, Faltermeier A: The influence of electron beams irradiation on colour stability and hardness of aesthetic brackets. Eur J Orthod, 34:427-431, 2012.
49. Douglas RD, Steinhauer TJ, Wee AG: Intraoral determination of the tolerance of dentists for perceptibility and acceptability of shade mismatch. J Prosthet Dent, 97:200-208, 2007.
50. Scabell AL, Elias CN, Fernandes DJ, Quintao CCA: Failure of fiber reinforced composite archwires. J Res Practice in Dent, Article ID 304484, doi: 10.5171/2013.304484, 2013.
51. Hamanaka I, Iwamoto M, Lassila L, Vallittu P, Shimizu H, Takahashi Y: Influence of water sorption on mechanical properties of injection-molded thermoplastic denture base resin. Acta Odontol Scand, 22:1-7, 2014.
52. Ardeshna AP. Clinical evaluation of fiber-reinforced-plastic bonded orthodontic retainers. Am J Orthod Dentofacial Orthop, 139:761-767, 2011.
53. Shiozawa M, Takahashi H, Asakawa Y, Iwasaki N: Color stability of adhesive resin cements after immersion in coffee. Clin Oral Investiq, doi: 10.1007/s00784-014-1272-8, 2014.
54. Dietschi D, Campanile G, Holz J, Meyer JM: Comparison of the color stability of ten new-generation composites: an in vitro study. Dent Mater, 10:353-362, 1994.
55. Lee IB, Min SH, Kim SY, Ferracane J: Slumping tendency and rheological properties of flowable composites. Dent Mater, 26:443-448, 2010.

56. Ertaş E, Güler AU, Yücel AÇ, Köprülü H, Güler E: Color stability of resin composites after immersion in different drinks. Dent Mater, 25:371-376, 2006.
57. Kloukos D, Pandis N, Eliades T: Bisphenol-A and residual monomer leaching from orthodontic adhesive resins and polycarbonate brackets: A systematic review. Am J Orthod Dentofacial Orthop, 143:104-112, 2013.
58. Kloukos D, Taoufik E, Eliades T, Katsaros C, Eliades G: Cytotoxic effects of polycarbonate-based orthodontic bracket by activation of mitochondrial apoptotic mechanisms. Dent Mater, 29:35-44, 2013.
59. Eliades T: Orthodontic materials research and applications: Part 2. Current status and projected future developments in materials and biocompatibility. Am J Orthod Dentofacial Orthop, 131:253-262, 2007.

Figure legends

Figure 1. Processing technique for manufacturing GFRP through pultrusion. (a) FE-SEM image of E-glass fibers used as a reinforcement for the GFRPs. Scale bars are equal to 10 μm. (b) Schematic illustration of the pultrusion process.

Figure 2. Photograph of frictional testing system.

Figure 3. Experimental set-up for color-stability measurement. (a) The GFRP sample devised for colorimetric measurement. This sample was prepared by arranging seven wire segments. Flowable resin was used to fix the wire segments. (b) Photograph of the sample and device set-up during measurement. The elastic tip of the instrument was in contact with the middle of the sample.

Figure 4. Apparent transparency of samples. (a) without sample, (b) with Ni-Ti-A, (c) with GFRP-13, and (d) with GFRP-7. Sample diameters are 0.45 mm (0.018 inch). Scale bars are equal to 1 mm.

Figure 5. FE-SEM images of the surface of four metallic wires and two GFRP wires. (a) SS; (b) Co-Cr; (c) β-Ti; (d) Ni-Ti-B; (e) GFRP-13; (f) GFRP-7. Scale bars are equal to 10 μm.

Figure 6. Three-dimensional SPM topography images (20 × 20 μm) of four metallic wires and two GFRP wires. (a) SS, R_a = 16.5 ± 8.9 nm; (b) Co-Cr, R_a = 17.1 ± 2.8 nm; (c) β-Ti, R_a = 69.3 ± 10.3 nm; (d) Ni-Ti-B, R_a = 10.7 ± 2.5 nm; (e) GFRP-13, R_a = 33.4 ± 8.3 nm; (f) GFRP-7, R_a = 20.2 ± 26.6 nm.

Figure 7. Dynamic hardness and elastic modulus of four metallic wires and two GFRP wires obtained by dynamic ultra-micro hardness test. (a) Dynamic hardness. (b) Elastic modulus. Values connected by horizontal bars with '*' are not significantly different from each other ($p > 0.05$).

Figure 8. Frictional force of four metallic wires and two GFRP wires against two types of bracket obtained by the frictional test. (a) Polymeric composite bracket. (b) Ceramic bracket. Values connected by horizontal bars with '*' are not significantly different from each other ($p > 0.05$).

Figure 9. Flexural properties of five metallic wires and two GFRP wires. (a) Flexural strength and (b) flexural modulus. Values connected by horizontal bars with '*' are not significantly different from each other ($p > 0.05$).

Figure 10. Typical load-deflection curves of five metallic wires and two GFRP wires. The middle portion of each wire was deflected to 1.95 mm and

then unloaded at the same speed.

Figure 11. Effect of thermal cycling on the flexural properties of GFRP wires. (a) GFRP-13 and (b) GFRP-7. No significant differences in flexural properties were observed after any number of cycles ($p > 0.05$).

Figure 12. FE-SEM images of the surface appearances of GFRP wires, before and after thermocycling of 1,200 times. (a) GFRP-13 before thermocycling, (b) GFRP-13 after thermocycling, (c) GFRP-7 before thermocycling, and (d) GFRP after thermocycling. Original magnification is 2,000x. Scale bars are equal to 10 μm.

Figure 13. Photograph of the GFRP wires before and after immersion in the coffee solution for 4 weeks. (a) GFRP-13 before immersion. (b) GFRP-7 before immersion. (c) GFRP-13 after immersion. (d) GFRP-7 after immersion. As indicated by the white arrows, the flowable resin that was used to fix the GFRP wires showed discoloration after immersion, while the GFRP wires themselves showed no discoloration.

Figure 14. Cytotoxicity to human gingival fibroblast culture. Mean control value was set to 100%, and all values were calculated as % of control. No significant differences in cytotoxicity were observed among all samples ($p > 0.05$).

Figure 15. Photographs of esthetic GFRP orthodontic archwires. (a) GFRP archwires for upper and lower arches (formed by putting straight wire into a curved aluminum mold and heating at 155°C, near the glass transition point of polycarbonate, for 120 min). (b) Photograph of esthetic GFRP orthodontic archwires. Laboratory GFRP archwires and commercially available polycarbonate brackets fixed to the teeth in the dental model.

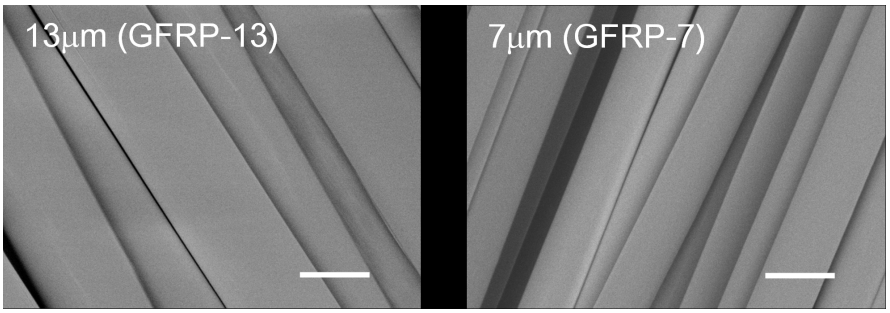

(a)

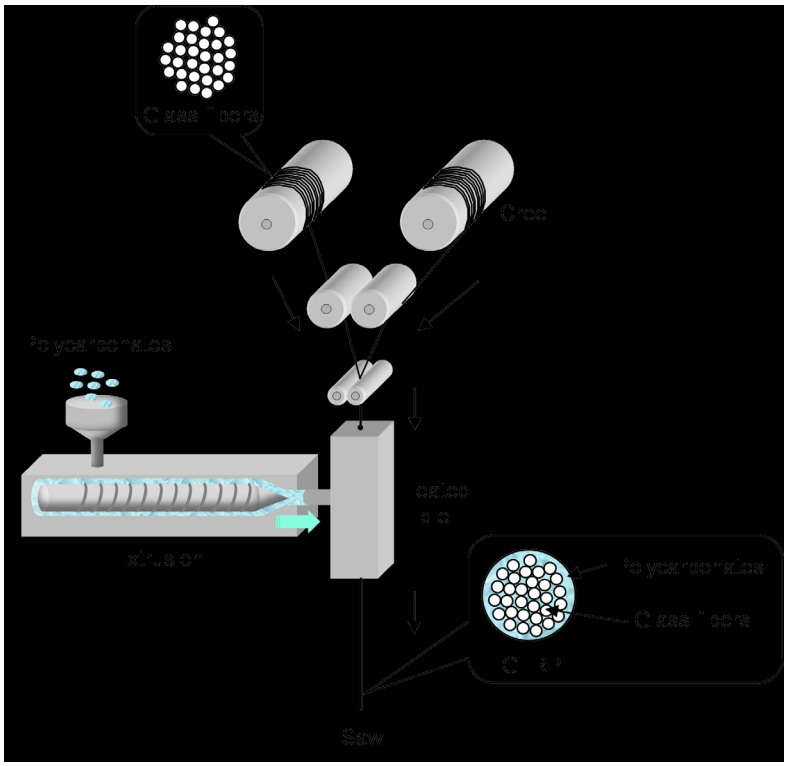

(b)

Figure 1

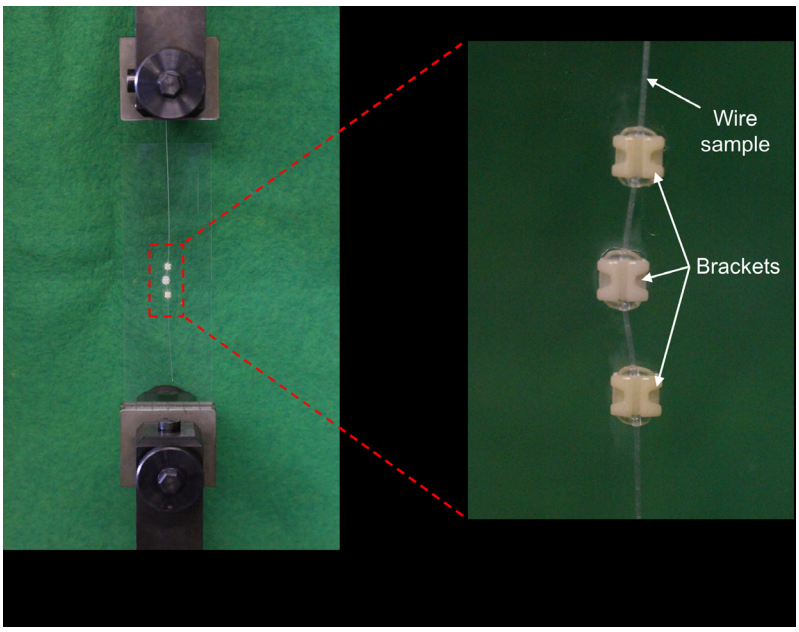

Figure 2

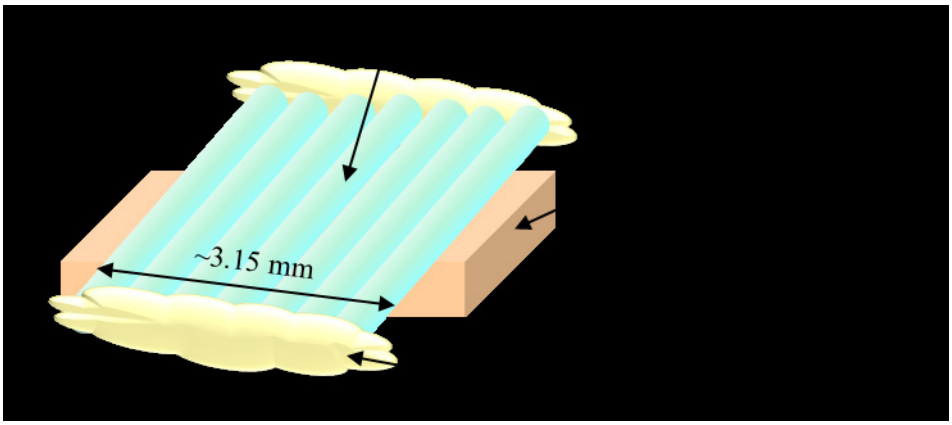

(a)

(b)

Figure 3

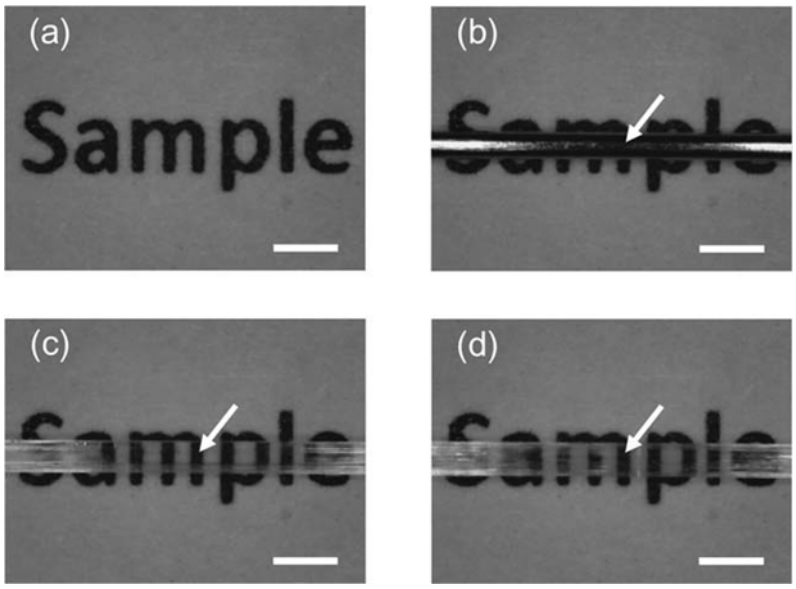

Figure 4

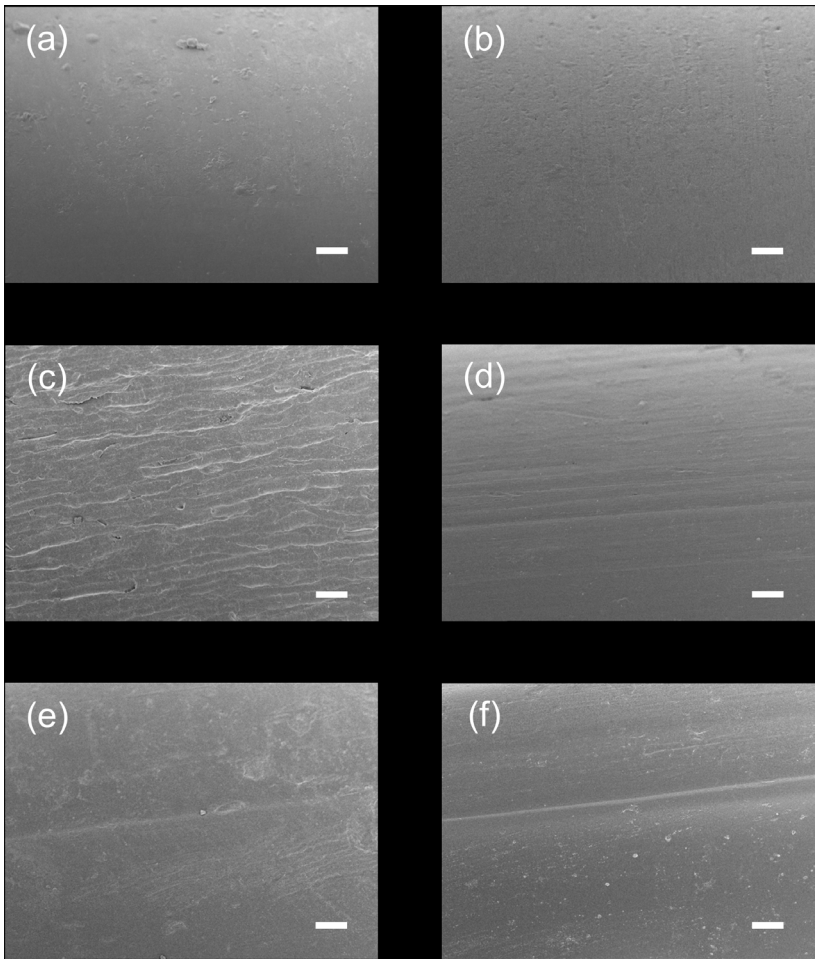

Figure 5

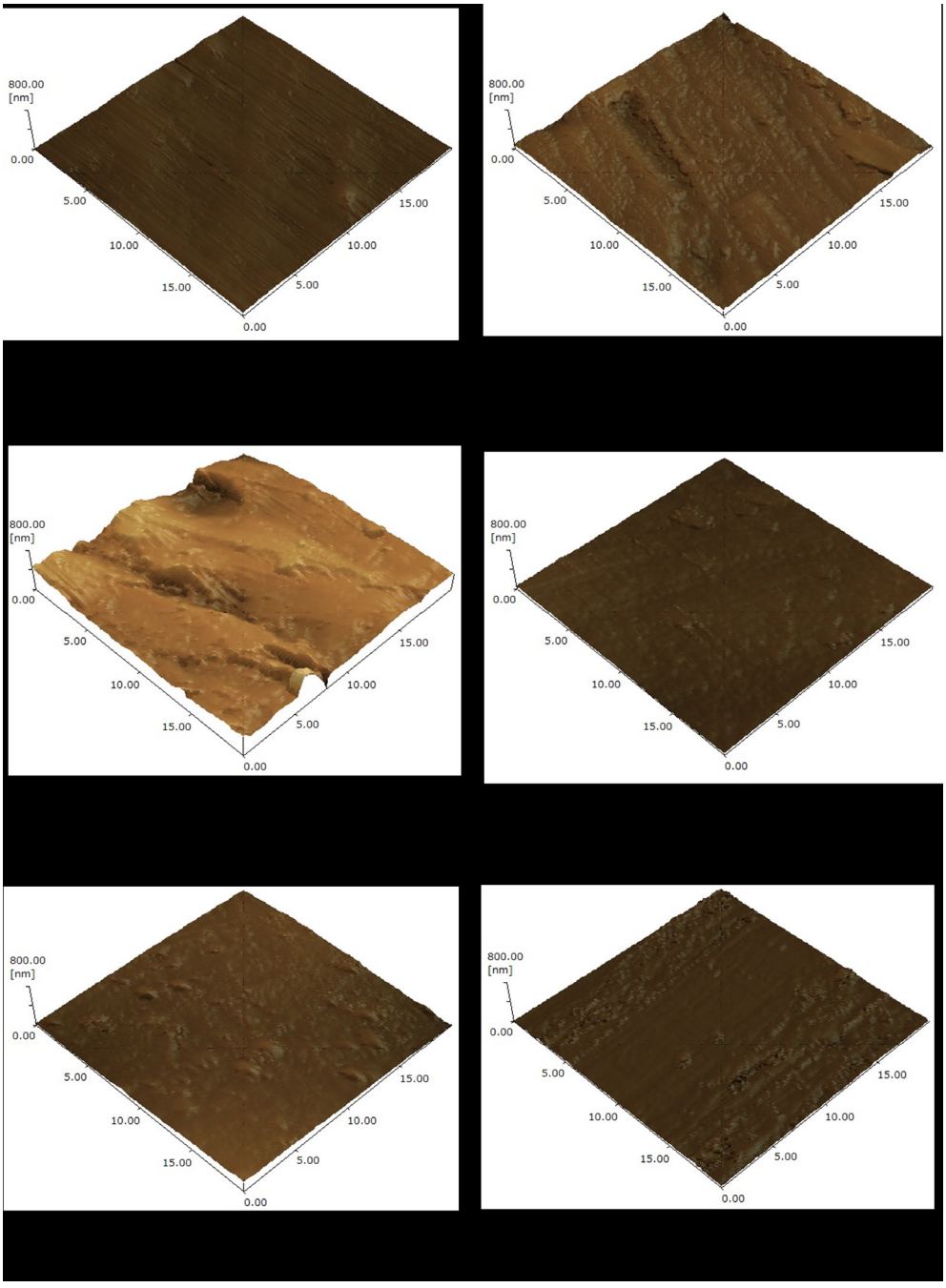

Figure 6

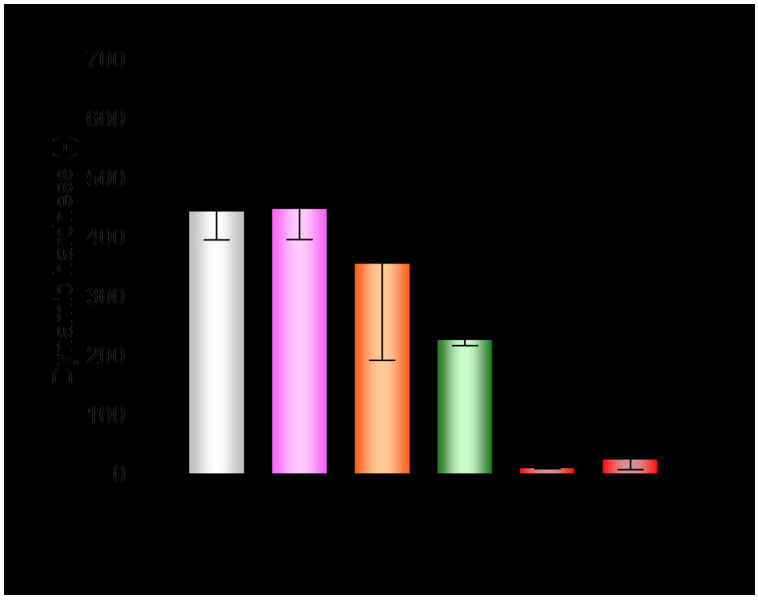
Dynamic hardness (-)
700
600
500
400
300
200
100
0

(a)

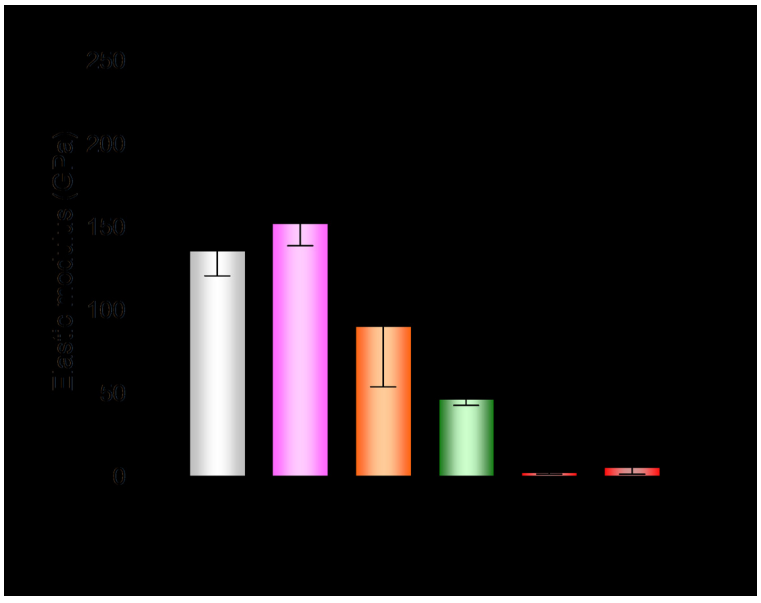
Elastic modulus (GPa)
250
200
150
100
50
0

(b)

Figure 7

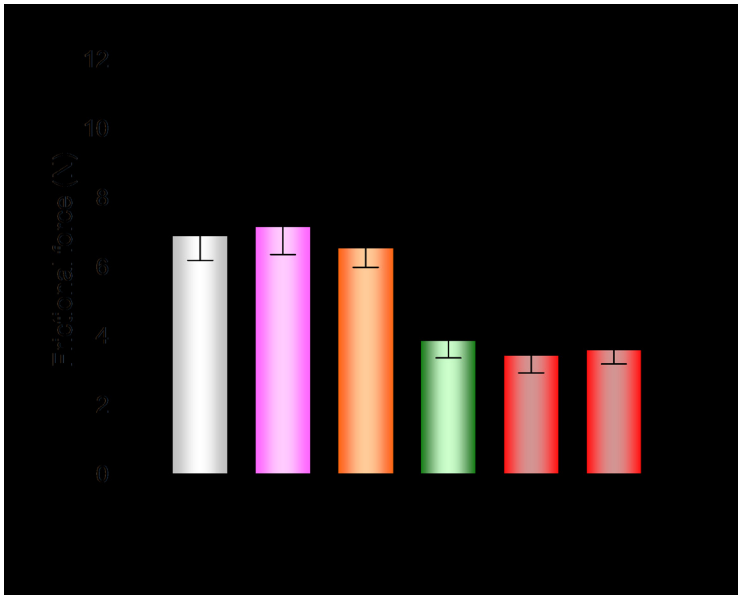
Frictional force (N)
0
2
4
6
8
10
12

(a)

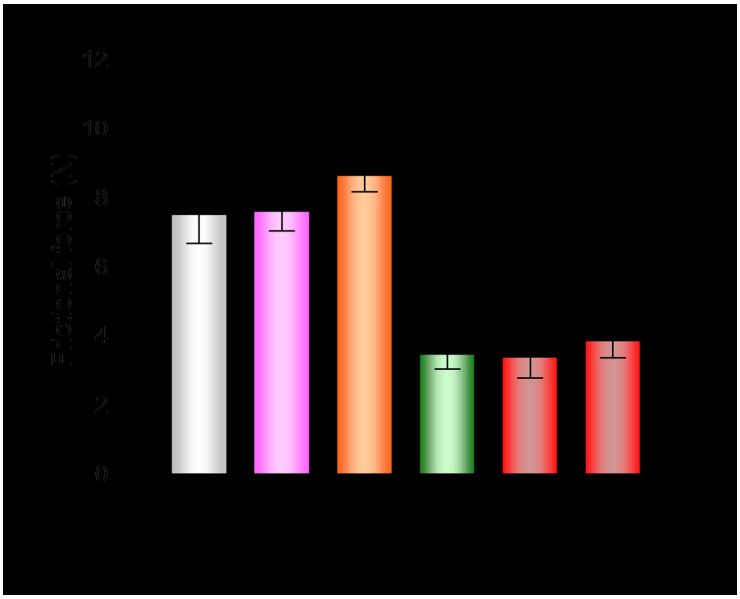
Frictional force (N)
0
2
4
6
8
10
12

(b)

Figure 8

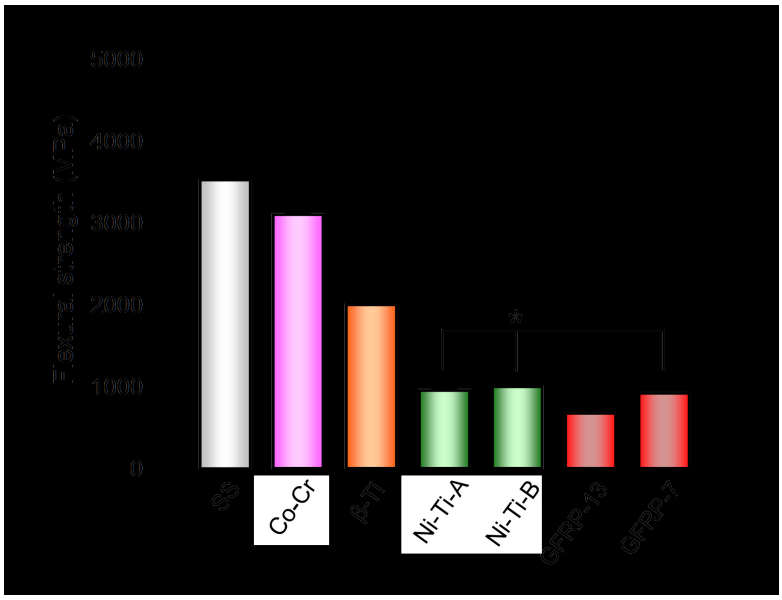
5000
4000
3000
2000
1000
0
SS
Co-Cr
β-Ti
Ni-Ti-A
Ni-Ti-B
GFRP-13
GFRP-7
*

(a)

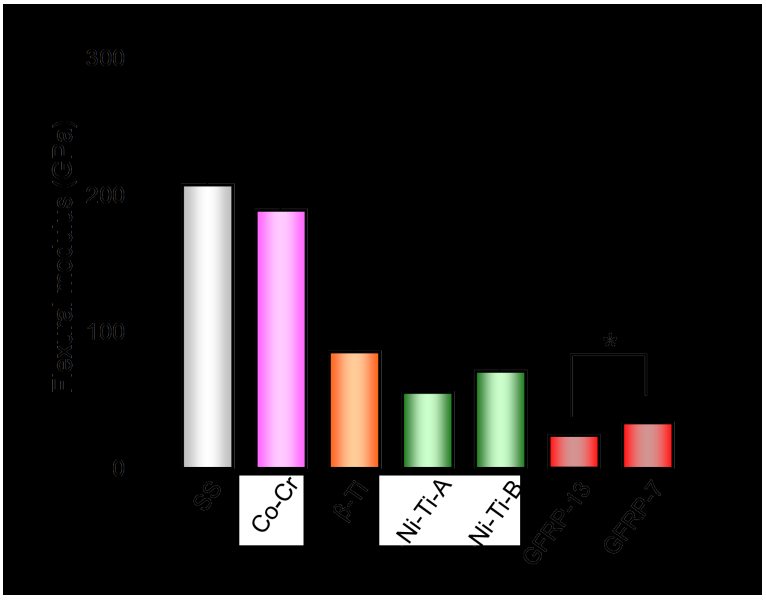
300
200
100
0
SS
Co-Cr
β-Ti
Ni-Ti-A
Ni-Ti-B
GFRP-13
GFRP-7
*

(b)

Figure 9

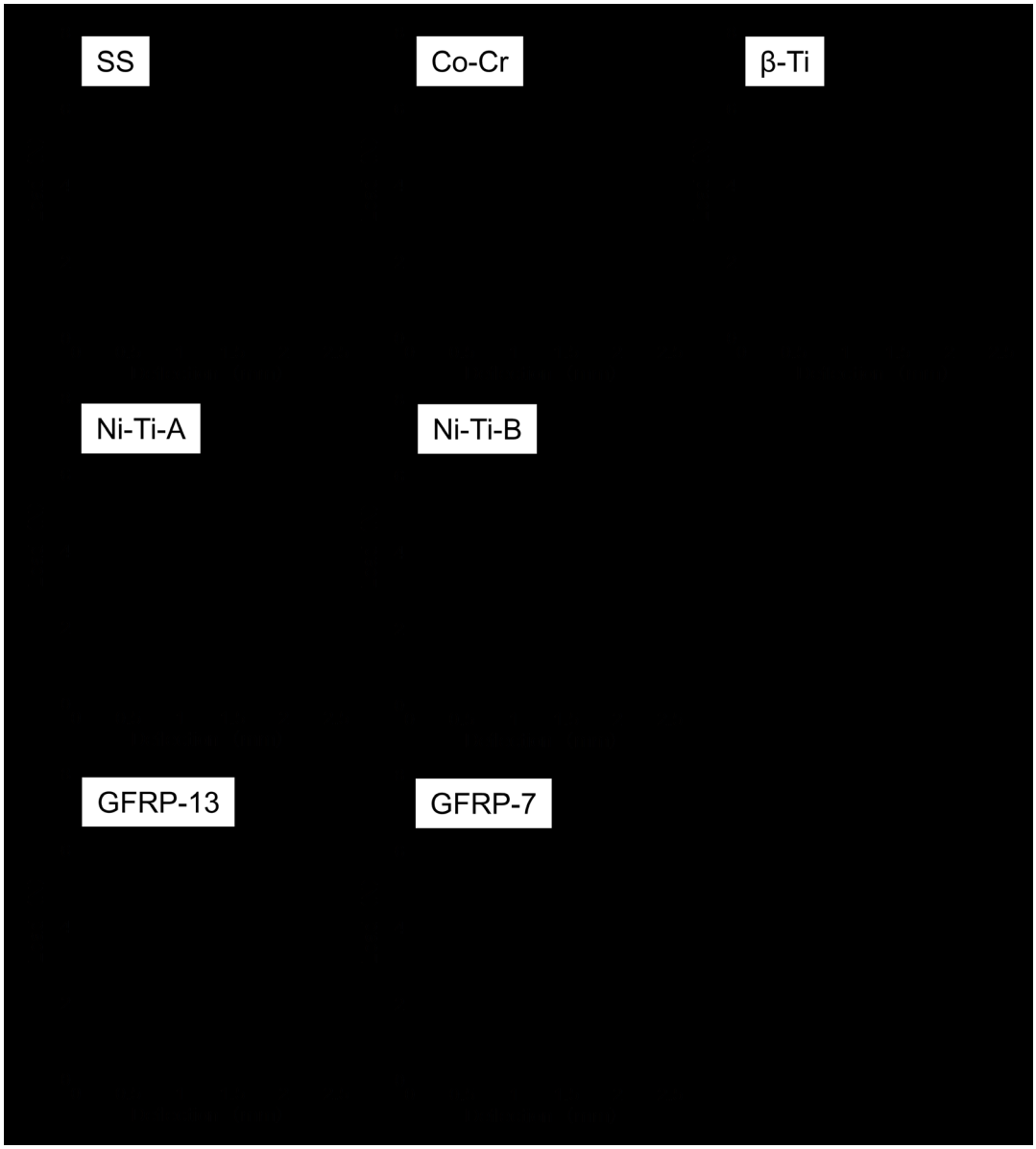

Figure 10

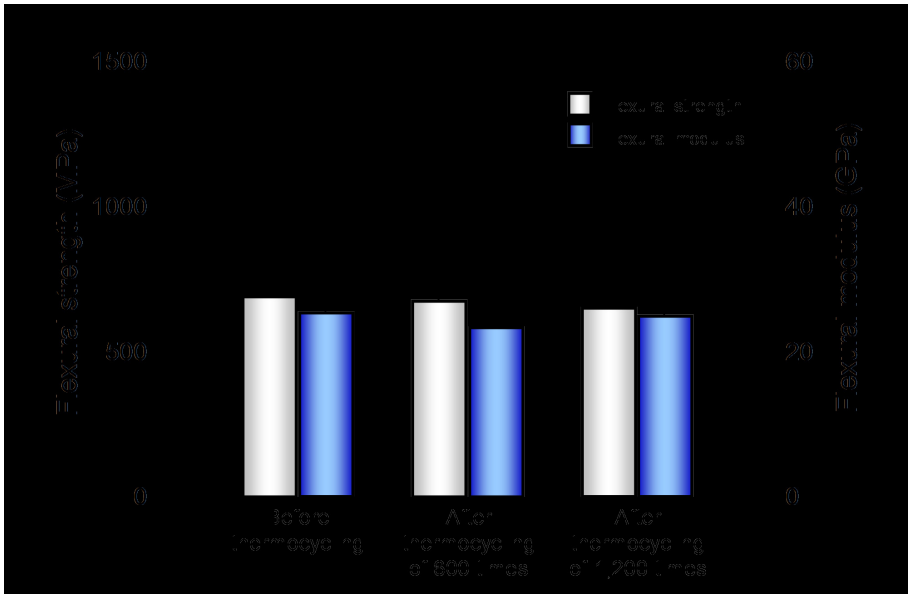

(a)

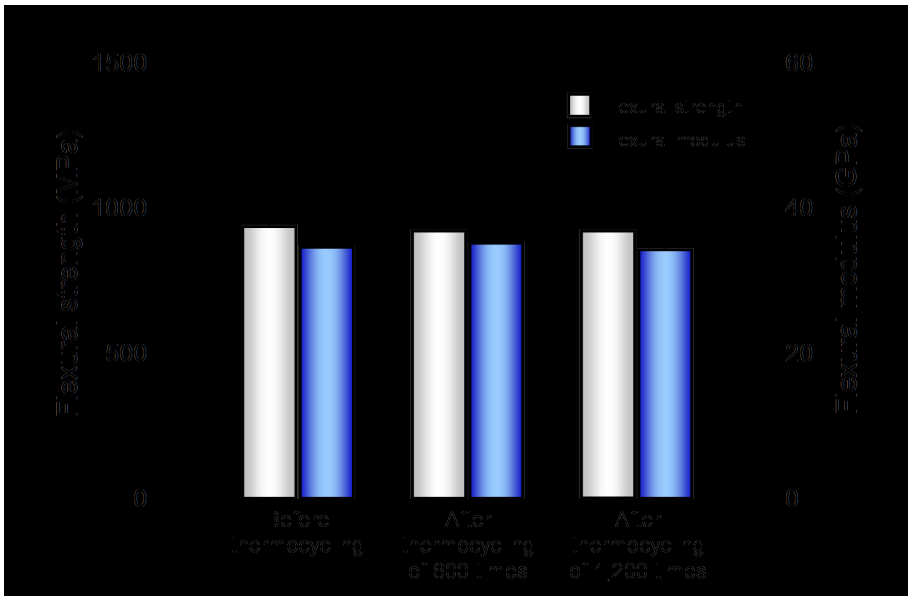

(b)

Figure 11

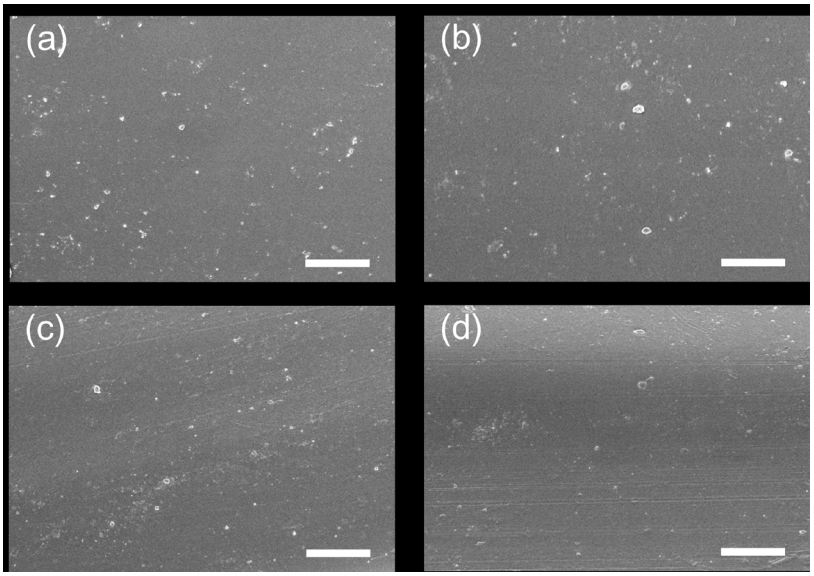

Figure 12

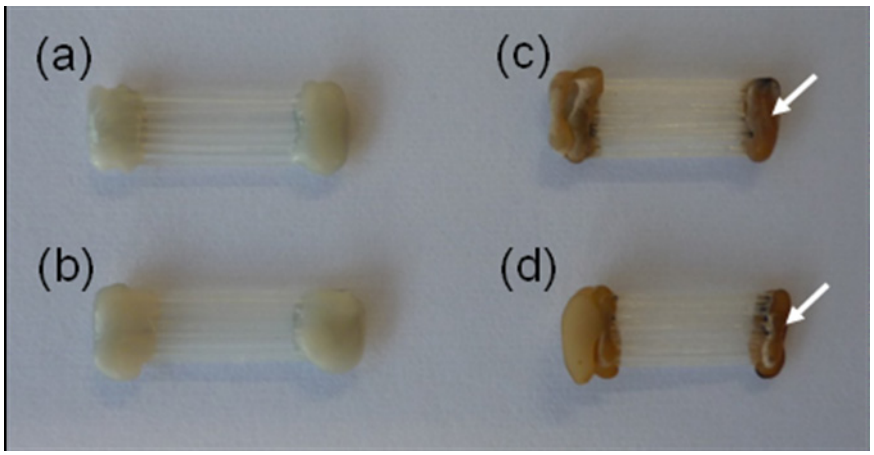

Figure 13

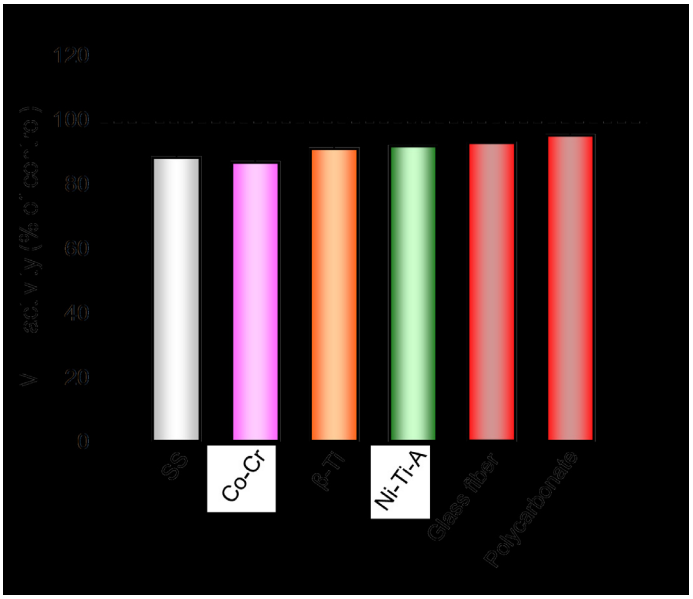
120
100
80
60
40
20
0
SS
Co-Cr
β-Ti
Ni-Ti-A
Glass fiber
Polycarbonate

Figure 14

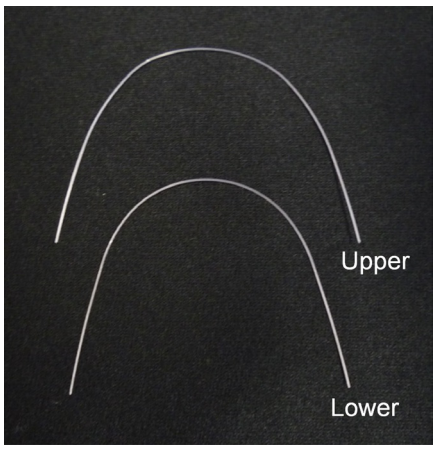

(a)

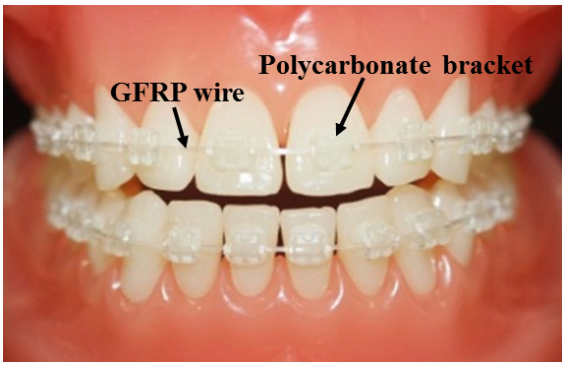

(b)

Figure 15

Code	Wire alloy	Wire Name	Composition (wt%)	Manufacturer
SS	Stainless steel	Stainless Steel	17.0-19.0% Cr, 8.0-10.0% Ni, 5%(C, Mn, P, S, Si) , balance mainly Fe	Ormco, Glendora, CA, USA
Co-Cr	Cobalt-chromium-nickel	Elgiloy® Red	40% Co, 20% Cr, 15.81% Fe, 15% Ni, 7% Mo, 2% Mn, 0.15% C, 0.01% Be maximum	Rocky mountain orthodontics, Denver, CO, USA
β-Ti	β-titanium	Bendaloy®	11.2% Mo, 6.26% Zr, 4.62% Sn, 0.32% Fe, 4.16% O, 1.42% C, 0.2% Cl, 71.7% Ti	Rocky mountain orthodontics, Denver, CO, USA
Ni-Ti-A	Nickel-titanium	Memory arch wire	55.0% Ni, 45.0% Ti	American Orthodontics, Sheboygan, WI, USA
Ni-Ti-B		Nickel Titanium Straight Length	54.5-57.0% Ni, 0.05% C maximum, 0.05% Co maximum, 0.01% Cu maximum, 0.01%Cr maximum, 0.005% H maximum, 0.05% Fe maximum, 0.025% Nb maximum, 0.05% O maximum, balanced mainly Ti	G&H Wire Co., Greenwood, IN, USA

NBS unit	Critical remarks of color differences	
0.0– 0.5	Trace	Extremely slight change
0.5– 1.5	Slight	Slight change
1.5– 3.0	Noticeable	Perceivable
3.0– 6.0	Appreciable	Marked change
6.0– 12.0	Much	Extremely marked change
12.0 or more	Very much	Change to other color

	24 hours		1 week		2 weeks		4 weeks	
	ΔE^*	NBS units	ΔE^*	NBS units	ΔE^*	NBS units	ΔE^*	NBS units
GFRP-7	1.10 ± 0.37	1.01 ± 0.34	0.98 ± 0.53	0.90 ± 0.49	0.97 ± 0.55	0.90 ± 0.51	0.62 ± 0.40	0.57 ± 0.36